BIOCHEMICAL PHARMACOLOGY 75 (2008) 1014–1026

available at www.sciencedirect.com

ScienceDirect

journal homepage: www.elsevier.com/locate/biochempharm

Synthesis and pharmacological evaluation of the novel *pseudo*-symmetrical tamoxifen derivatives as anti-tumor agents

Isamu Shiina [a,*], *Yoshiyuki Sano* [a], *Kenya Nakata* [a], *Takaaki Kikuchi* [a], *Akane Sasaki* [a], *Masahiko Ikekita* [b,*], *Yukitoshi Nagahara* [b], *Yoshimune Hasome* [b], *Takao Yamori* [c,*], *Kanami Yamazaki* [c]

[a] *Department of Applied Chemistry, Faculty of Science, Tokyo University of Science, Kagurazaka, Shinjuku-ku, Tokyo 162-8601, Japan*

[b] *Department of Applied Biological Science, Faculty of Science and Technology, Tokyo University of Science, Yamazaki, Noda, Chiba 278-8510, Japan*

[c] *Division of Molecular Pharmacology, Cancer Chemotherapy Center, Japanese Foundation for Cancer Research, Ariake, Koto-ku, Tokyo 135-8550, Japan*

ARTICLE INFO

Article history:
Received 4 June 2007
Accepted 13 November 2007

Keywords:
Cancer
Tamoxifen
Symmetrical derivatives
HL-60
Panel of cancer cell lines
JFCR 39

ABSTRACT

Four *pseudo*-symmetrical tamoxifen derivatives, RID-B (**13**), RID-C (**14**), RID-D (**15**), and bis(dimethylaminophenetole) (**16**), were synthesized via the novel three-component coupling reaction, and the structure–activity relationships of these *pseudo*-symmetrical tamoxifen derivatives were examined. It was discovered that **13** and **16** strongly inhibit the viability of the HL-60 human acute promyelocytic leukemia cell line, whereas **14** possesses a medium activity against the same cell line and **15** has no effect on the cell viability. The global anti-tumor activity of **13–16** against a variety of human cancer cells was assessed using a panel of 39 human cancer cell lines (JFCR 39), and it was shown that RID-B (**13**) strongly inhibited the growth of several cancer cell lines at concentrations of less than 1 μM (at 0.38 μM for SF-539 [central nervous system], at 0.58 μM for HT-29 [colon], at 0.20 μM for DMS114 [lung], at 0.21 μM for LOX-IMVI [melanoma], and at 0.23 μM for MKN74 [stomach]).

1. Introduction

Tamoxifen (**1**), the early generation of SERMs (selective estrogen receptor modulators), has been used as the first-line agent for the treatment of estrogen-dependent breast cancer since the 1970s [1–7]. The accumulative risk-benefit assessment of tamoxifen therapy and comparative studies of **1** and other new types of drugs also established its efficacy and safety (Fig. 1). Therefore, the development of an expeditious synthetic route for producing new tamoxifen-type drugs followed by the systematic studies of their biological activities are significantly required.

In this paper, we report a novel short-step synthesis of a new class of anti-cancer agents, which are *pseudo*-symmetrical tamoxifen derivatives RID-B (**13**), RID-C (**14**), RID-D (**15**), and bis(dimethylaminophenetole) (**16**), via the three-component coupling reaction [8]. Their cytotoxic activity against HL-60 human acute promyelocytic leukemia and growth inhibition activity of **13–16** against a panel of 39 human cancer cell lines were also evaluated.

* *Corresponding author*. Tel.: +81 3 3260 4271; fax: +81 3 3260 5609.
E-mail addresses: shiina@rs.kagu.tus.ac.jp (I. Shiina), masalab@rs.noda.tus.ac.jp (M. Ikekita), yamori@jfcr.or.jp (T. Yamori).
0006-2952/$ – see front matter
doi:10.1016/j.bcp.2007.11.005

2. Materials and methods

2.1. Materials and chemicals

Recently, we established a novel three-component coupling reaction among aromatic aldehydes, cinnamyltrimethylsilane (**5**), and aromatic nucleophiles in the presence of a Lewis acid catalyst as shown in Scheme 1 [9,10]. Furthermore, we reported that the sequential one-pot allylation and Friedel-Crafts type alkylation reaction can be effectively applied to the preparation of tamoxifen (**1**) and its halogenated derivatives [11,12]. For example, the coupling reaction of benzaldehyde, cinnamyltrimethylsilane (**5**), and anisole afforded the corresponding 3,4,4-triarylbutene, which is the basic skeleton of **1**, in a satisfactory yield.

Based on the preliminary results for the synthesis of tamoxifen (**1**) [11], droloxifene (**2**) [13], nafoxidine (**3**) and lasofoxifene (**4**) [14], the facile preparation of *pseudo*-symmetrical tamoxifen analogues was carried out using the three-component coupling reaction (**5** + **6** + anisole) to produce the coupling product **7** in high yield (Scheme 1). Bisphenol **8** [15–23] was prepared from **7** by heating with an excess amount of *t*-BuOK in DMSO via the base-catalyzed double-bond migration reaction and successive deprotection of the *O*-methyl group by BBr_3 in CH_2Cl_2 at 0 °C. Next, **8** was treated with 60% NaH followed by an excess amount of 2-pyrrolidinoethylchloride hydrochloric acid salt (**9**), 2-piperidinoethylchloride hydrochloric acid salt (**10**), 2-morphorinoethylchloride hydrochloric acid salt (**11**), or 2-dimethylaminoethylchloride hydrochloric acid salt (**12**) in DMF to afford the novel tamoxifen derivative, RID-B (**13**), RID-C (**14**), RID-D (**15**), or bis(dimethylaminophenetole) (**16**) [24], respectively.

It is well known that the *E*-isomer of tamoxifen is not anti-estrogenic, but functions as an estrogen agonist, although (*Z*)-tamoxifen is effective in treating estrogen-dependent breast cancer. Therefore, the efficiency of the synthesis of the tamoxifen derivatives usually depends on the stereoselectivity of the olefination step to generate the desired *Z*-isomer; however, it is not required to use stereogenic reactions to produce the *pseudo*-symmetrical system included in **13–16**.

2.2. HL-60 human acute promyelocytic leukemia

The HL-60 cells were supplied by the Cell Resource Center for Biomedical Research, Tohoku University (Sendai, Japan). The cells were maintained at 37 °C with 5% CO_2 in RPMI 1640 medium supplemented with kanamycin sulfate (64 mg/L), 2-mercaptoethanol (3.5 μL/L), sodium bicarbonate (2 g/L), and heat-inactivated 10% (v/v) fetal bovine serum. The cells were diluted with the medium to the constant concentrations of 4.0×10^5 cells/mL.

2.3. MTT assay

HL-60 cells were incubated in 96-well plates at 37 °C, and then, 11 μL of 20 mg/mL 3-(4,5-dimethylthiazol-2-yl)-2,5-diphenyl tetrazolium bromide (MTT; Sigma) in phosphate-buffered saline (PBS) was added to each well. The plates were incubated at 37 °C for 1 h. The plates were centrifuged at 350 × *g* for 5 min, the supernatants were discarded, and 100 μL of DMSO was added to dissolve the MTT formazan. The absorbance of each well was measured using a microplate reader at 570 nm. The percentage of cell viability was taken as the percent absorbance at 570 nm for the RID-treated cells and control.

2.4. A panel of 39 human cell lines (JFCR 39)

The panel of 39 human cancer cell lines (termed JFCR 39) [25–30] and B16F10 melanoma cells [31] were previously described. All cell lines were cultured in RPMI 1640 medium supplemented with 5% fetal bovine serum, penicillin (100 U/mL), and streptomycin (100 μg/mL) at 37 °C in humidified air containing 5% CO_2. The cell lines OVCAR3, A549, PC-3, and WiDr, which were used for the in vitro detailed analysis, originated from an ovarian cancer, non-small-cell lung cancer, prostate cancer, and colon cancer, respectively.

2.5. Analysis of cell proliferation inhibition

The inhibition of cell proliferation was assessed by measuring the changes in the total cellular protein in a culture of each cell line in the JFCR panel of the cell lines after 48 h of drug treatment using the a sulforhodamine B assay [32]. The 50% growth inhibition (GI_{50}) value of **13–16** was calculated as previously described [25–30]. The graphic representation of a drug's mean differential growth inhibition for the cell line panel was based on a calculation that used a set of GI_{50} values, as previously described [33–35]. To analyze the correlation between the mean graphs of drug A and drug B, the COMPARE computer algorithm was developed as previously described by Paull and co-workers [33] and Paull et al. [34]. The Pearson correlation coefficient between the mean graphs of drug A and drug B was also calculated (n = 39).

2.6. Statistical analysis

Pearson correlation coefficients were calculated for the COMPARE analysis and statistical correlation. To evaluate

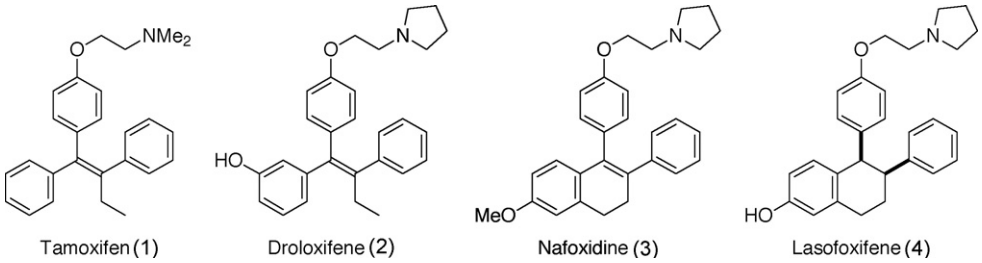

Fig. 1 – Structures of tamoxifen (1), droloxifene (2), nafoxidine (3), and lasofoxifene (4).

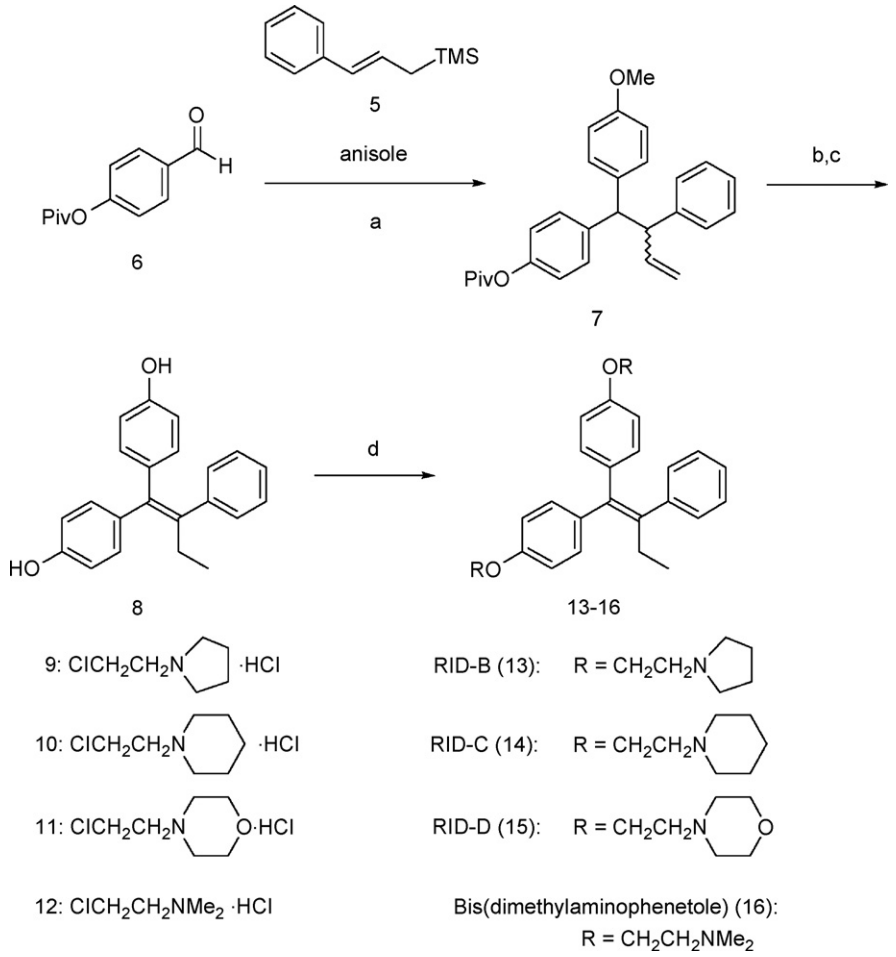

Scheme 1 – Reagents and conditions: (a) 5, $HfCl_4$ (1 equiv.), anisole, rt, 2 h, 78%; (b) *t*-BuOK, DMSO, 90 °C, 1 h, 93%; (c) BBr_3, CH_2Cl_2, 0 °C, 2 h, 86%; (d) NaH, 9, DMF, 50 °C, 30 min, 84% (for 13); NaH, 10, DMF, 50 °C, 30 min, 95% (for 14); NaH, 11, DMF, 50 °C, 30 min, 95% (for 15); NaH, 12, DMF, 50 °C, 30 min, 95% (for 16).

the statistical significance of the anti-tumor efficacy of **13–16**, the two-sided Mann–Whitney *U*-test was used in relative tumor growth ratio on 4, 7, 11, and 14 days. The number of samples is indicated in the description of each experiment. All statistical tests were two-sided.

3. Results

3.1. *Biological activity of the pseudo-symmetrical tamoxifen derivatives*

The potency of the anti-tumor activities of **13–16** were assessed in this study. In order to evaluate the anti-tumor activities of these newly prepared compounds against the HL-60 human acute promyelocytic leukemia, we tried to determine the efficiency of the *pseudo*-symmetrical compounds decreasing the cell viability by the MTT (3-(4,5-dimethyl-2-thiazolyl)-2,5-diphenyltetrazolium bromide) assay, a method of determining cell viability by measuring the mitochondrial succinic dehydrogenase activity.

The effects of tamoxifen (**1**), idoxifene, RID-B (**13**), and bis(dimethylaminophenetole) (**16**) on growth of the HL-60 human cell line were first measured by the MTT assay after a 4-h incubation (Fig. 2). A treatment of the HL-60 cells with 5 μg/mL of **1** gave *ca.* 50% of the final viability of the inhibited cells compared with the cell viability at 0 h. On the other hand, the biological activities of 5 μg/mL of **13** and **16** are strong enough to inhibit the cell viability in more than 90% of the content under the same conditions.

We next investigated the effects on the time-dependent viability of the HL-60 cells treated with **13–16** at various concentrations for 0–6 h (Fig. 3). RID-B (**13**) and bis(dimethylaminophenetole) (**16**) in the final concentrations of 5, 7.5, and 10 μM decreased the cell viability in a time-dependent manner. A 6-h incubation with 5, 7.5, and 10 μM final concentrations of **13** inhibited the cell viability more than 90% as measured by the MTT assay. RID-C (**14**) in 7.5 and 10 μM concentrations inhibited the cell viability more than 80% after a 6-h treatment, whereas **16** in 7.5 and 10 μM concentrations also inhibited the cell viability more than 90% under the same conditions. On the other hand, RID-D (**15**) showed no affect on the viability of the HL-60 cells after 6 h. Among them, **13**, **14**, and **16** clearly induced, dose-dependently, cell death to a greater extent than **15** as shown in Fig. 3. The median growth-inhibitory concentrations

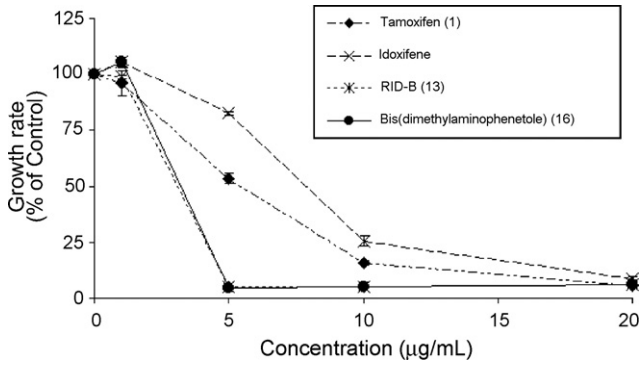

Fig. 2 – Effects of tamoxifen (1), idoxifene, RID-B (13), and bis(dimethylaminophenetole) (16) on the cell viability after a 4-h incubation. The dose-dependent effects of 1, idoxifene, 13, and 16 to HL-60 cells were measured by the MTT assay. The cell viability obtained from the absorbance of formazan at 0 h was 100%.

(IC_{50}) against the HL-60 cells after a 6-h incubation with **13** and **14** were calculated as 3 and 5 μM, respectively. Although **13**, **14**, and **16** have strong cytotoxic activities inducing apoptosis of the HL-60 cells, **15** containing the morpholine side chain shows no activity on the same cells. According to other reports on the effects of the structure variation of the side chain [36–38], it is indicated that oxygen in the morpholine side chain varied the cytotoxic characters of **13**, **14**, and **16** to no-cytotoxic by lowering its basicity.

3.2. *Cytotoxicity evaluated by the human cancer cell line panel assay*

An efficient screening system for the discovery of new anti-tumor agents using cultured human cancer cell lines was developed by a group at the National Cancer Institute in the early 1990s [33,34]. Furthermore, we established the original disease-oriented cancer cell line panel that consisted of 39 human cancer cell lines, 5 breast, 6 central nervous system, 5 colon, 7 lung, 1 melanoma, 5 ovarian, 2 kidney, 6 stomach, and 2 prostate cancers. We have a database including the growth-inhibitory parameters of more than 200 standard agents, most of which are anti-cancer drugs and various types of inhibitors. An effective method was established to compare standard drugs with each other for the mean graph pattern using the COMPARE Program and to confirm that drugs sharing a certain mode of action clustered together, as described previously [25–30]. Figs. 4–7 showed the dose-dependent viability of human cancer cell lines treated with RID-B (**13**), RID-C (**14**), RID-D (**15**), and bis(dimethylaminophenetole) (**16**), respectively. These results indicated that the new compounds had appreciable cytotoxic activities against the human cancer cell lines, and the results of evaluation of their anti-tumor activities are summarized in Table 1 accompanied with four calculated parameters (log GI_{50}, MG-MID, Delta, and Range).

The GI_{50} value, the molar concentration of testing compounds for inhibition of cell growth at 50% compared to the control, was calculated as $100 \times [(T - T_0)/(C - T_0)] = 50$. The absorbance ($C$, T, or T_0) for the control well, the test wells, or the test wells at time 0 (addition of the testing samples) was measured at 525 nm. The TGI value, the molar concentration

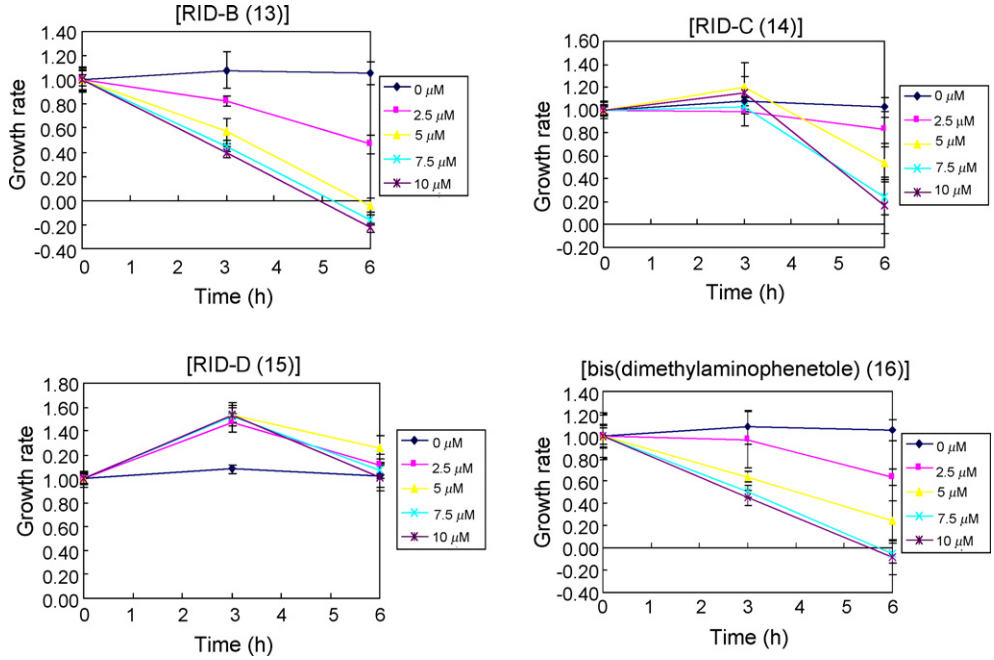

Fig. 3 – Effects of RID-B (13), RID-C (14), RID-D (15), and bis(dimethylaminophenetole) (16) on growth of cells. Time-dependent effects of 13–16 on HL-60 cells were measured by the MTT assay. The cell viability obtained from the absorbance of formazan at 0 h was 100%. Error bars show S.D. (n = 5). HL-60 cells were treated at the following four different final concentrations: 2.5, 5, 7.5 and 10 μM, respectively.

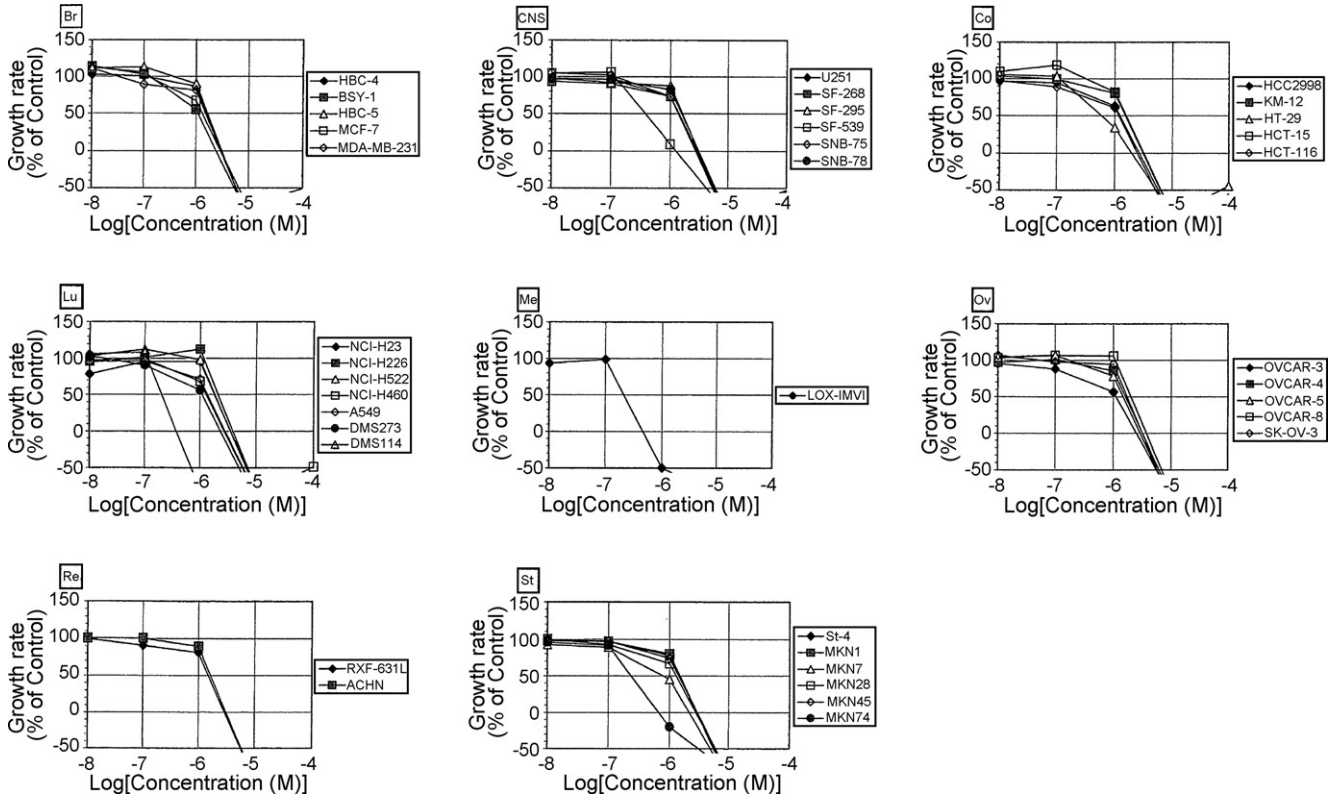

Fig. 4 – Growth inhibition against a panel of human cancer cell lines. Dose-dependent effects of RID-B (13) on each cancer cell were measured as described in Section 2.

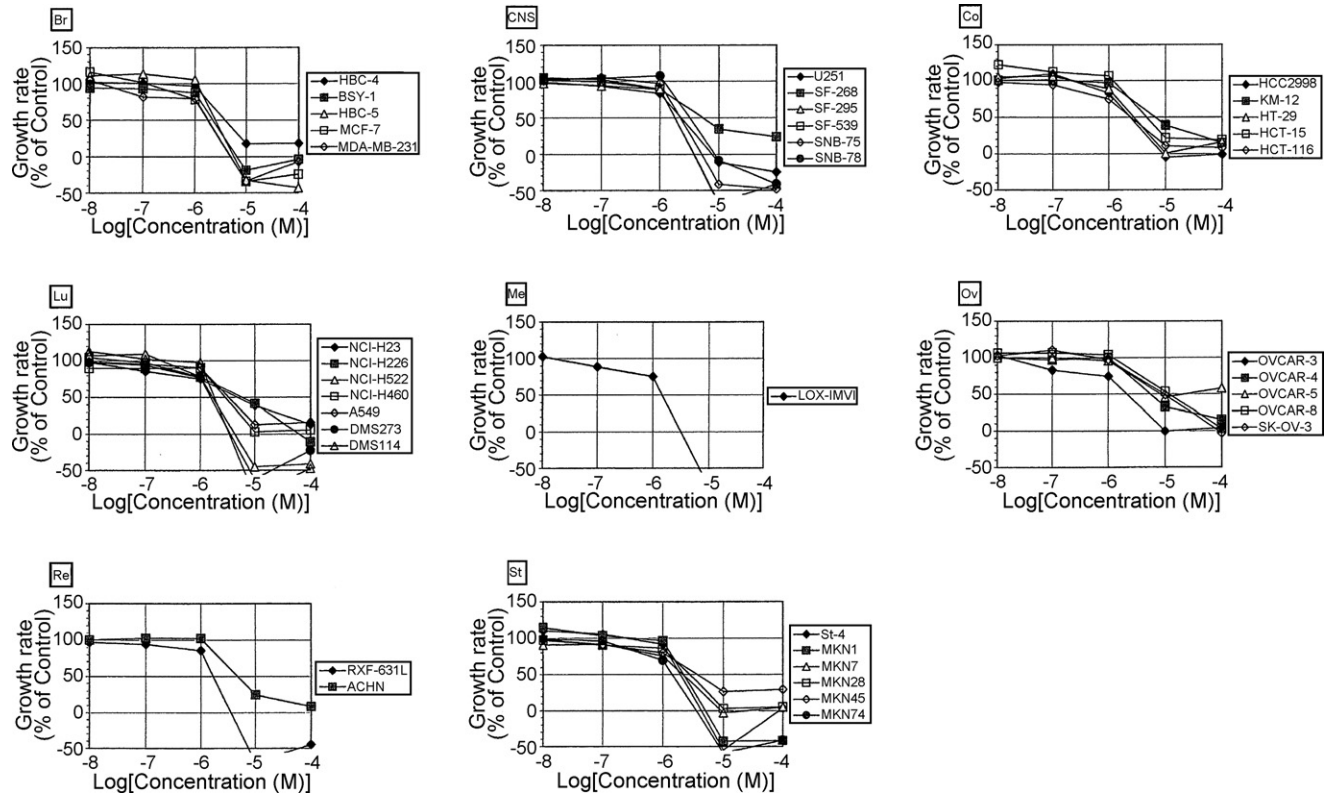

Fig. 5 – Growth inhibition against a panel of human cancer cell lines. Dose-dependent effects of RID-C (14) on each cancer cell were measured as described in Section 2.

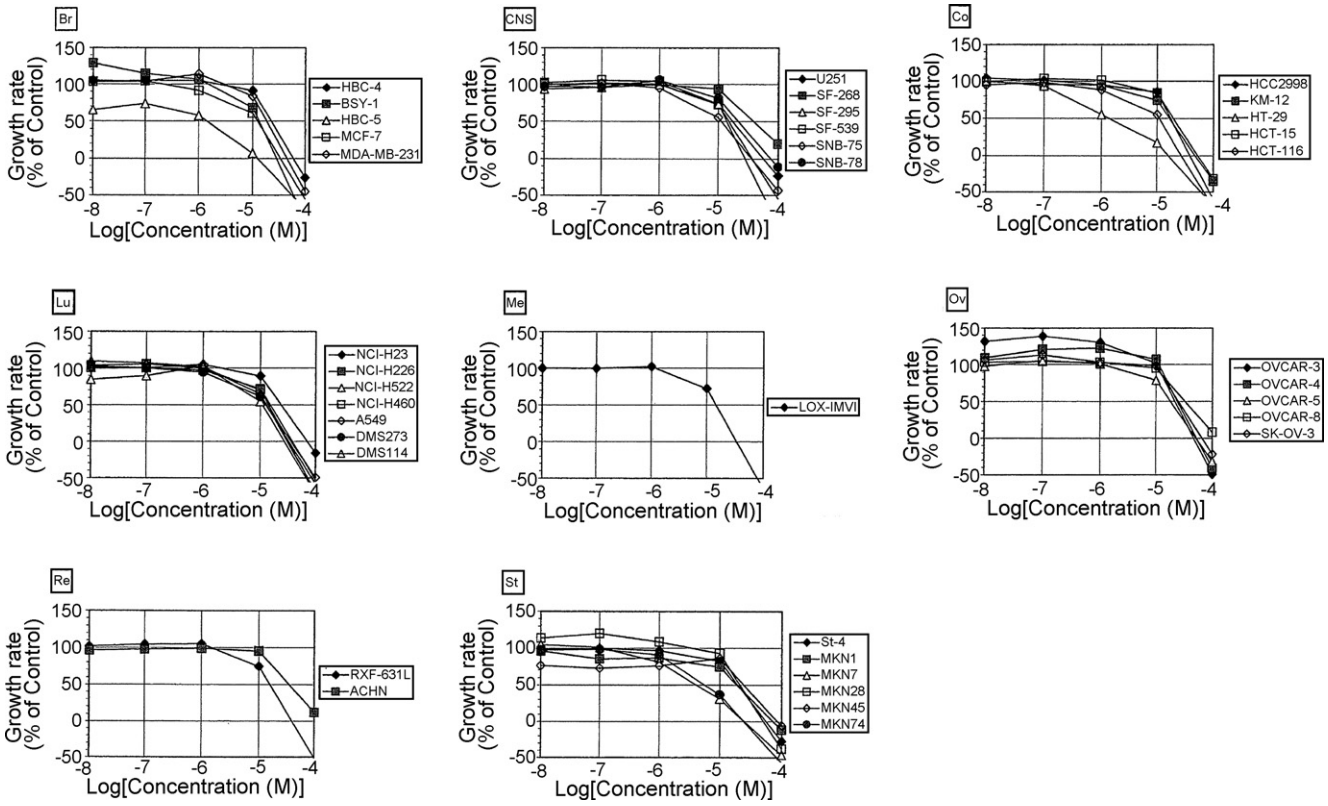

Fig. 6 – Growth inhibition against a panel of human cancer cell lines. Dose-dependent effects of RID-D (15) on each cancer cell were measured as described in Section 2.

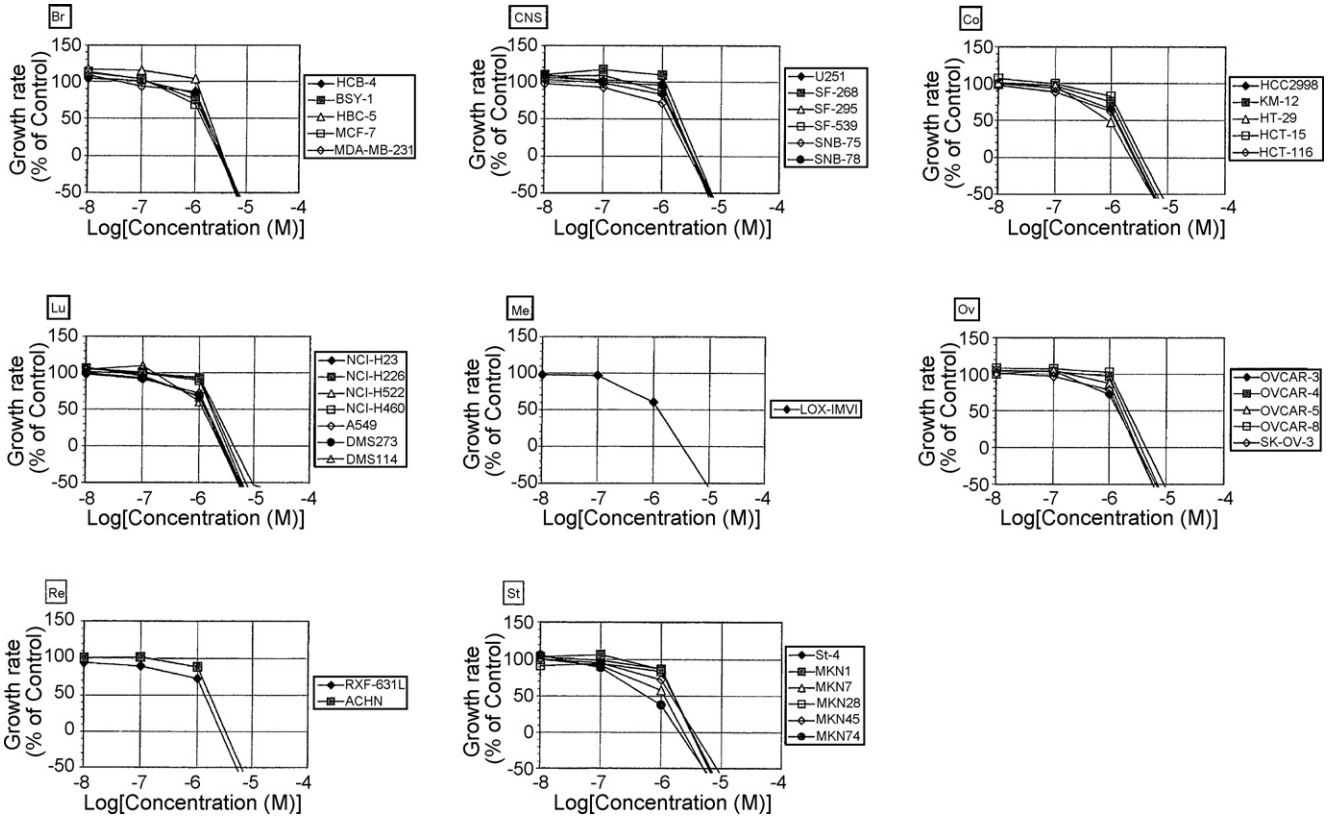

Fig. 7 – Growth inhibition against a panel of human cancer cell lines. Dose-dependent effects of bis(dimethylaminophenetole) (16) on each cancer cell were measured as described in Section 2.

Table 1 – Summary of human cancer cell line panel assay of *pseudo*-symmetrical tamoxifens 13–16

Origin of cancer	Cell line	RID-B (**13**)		RID-C (**14**)		RID-D (**15**)		Bis(dimethylaminophenetole) (**16**)	
		Log GI_{50} (M)[a]	(MG-MID) −log GI_{50}	Log GI_{50} (M)[a]	(MG-MID) −log GI_{50}	Log GI_{50} (M)	(MG-MID) −log GI_{50}	Log GI_{50} (M)	(MG-MID) −log GI_{50}
Breusl	HBC-4	−5.80	−0.13	−5.41	−0.05	−4.65	−0.19	−5.80	−0.03
	BSY-1	−5.96	0.03	−5.65	0.19	−4.88	0.04	−5.83	0.00
	HBC-5	−5.78	−0.15	−5.60	0.14	−5.85	1.01	−5.72	−0.11
	MCF-7	−5.88	−0.05	−5.75	0.29	−4.91	0.07	−5.87	0.04
	MDA-MB-231	−5.81	−0.12	−5.74	0.28	−4.74	−0.10	−5.78	−0.05
Central nervous system	U251	−5.86	−0.07	−5.65	0.19	−4.75	−0.09	−5.79	−0.04
	SF-268	−5.85	−0.08	−5.28	−0.18	−4.41	−0.43	−5.68	−0.15
	SF-295	−5.79	−0.14	−5.75	0.29	−4.82	−0.02	−5.75	−0.08
	SF-539	−6.42	0.49	−5.75	0.29	−4.86	0.02	−5.77	−0.06
	SNB-75	−5.86	−0.07	−5.66	0.20	−4.95	0.11	−5.86	0.03
	SNB-78	−5.81	−0.12	−5.50	0.04	−4.66	−0.18	−5.75	−0.08
Colon	IICC2998	−5.91	−0.02	−5.62	0.16	−4.76	−0.08	−5.90	0.07
	KM-12	−5.82	−0.11	−5.18	−0.28	−4.78	−0.06	−5.84	0.01
	HT-29	−6.23	0.30	−5.56	0.10	−5.86	1.02	−6.04	0.21
	HCT-15	−5.81	−0.12	−5.33	−0.13	−4.71	−0.13	−5.78	−0.05
	HCT-116	−5.93	0.00	−5.61	0.15	−4.96	0.12	−5.92	0.09
Lung	NC1-H23	−5.74	−0.19	−5.31	−0.15	−4.63	−0.21	−5.70	−0.13
	NC1-H226	−5.67	−0.26	−5.23	−0.23	−4.85	0.01	−5.74	−0.09
	NCI-II522	−5.73	−0.20	−5.77	0.31	−4.96	0.12	−5.89	0.06
	NCI-H460	−5.88	−0.05	−5.54	0.08	−4.82	−0.02	−5.77	−0.06
	A549	−5.86	−0.07	−5.48	0.02	−4.90	0.06	−5.86	0.03
	DMS273	−5.96	0.03	−5.81	0.35	−4.90	0.06	−5.89	0.06
	DMS114	−6.69	0.76	−5.74	0.28	−4.89	0.05	−5.93	0.10
Melanoma	LOX-IMVI	−6.67	0.74	−5.83	0.37	−4.84	0.00	−5.91	0.08
Ovary	OVCAR-3	−5.96	0.03	−5.67	0.21	−4.66	−0.18	−5.85	0.02
	OVCAR-4	−5.79	−0.14	−5.26	−0.20	−4.62	−0.22	−5.73	−0.10
	OVCAR-5	−5.83	−0.10	−4.00	−1.46	−4.74	−0.10	−5.79	−0.04
	OVCAR-8	−5.70	−0.23	−4.93	−0.53	−4.48	−0.36	−5.67	−0.16
	SK-OV-3	−5.77	−0.16	−5.02	−0.44	−4.60	−0.24	−5.83	0.00
Kidney	RXF-631L	−5.82	−0.11	−5.77	0.31	−4.81	−0.03	−5.87	0.04
	ACHN	−5.78	−0.15	−5.32	−0.14	−4.46	−0.38	−5.77	−0.06
Stomach	St-4	−5.84	−0.09	−5.72	0.26	−4.70	−0.14	−5.78	−0.05
	MKNI	−5.83	−0.10	−5.67	0.21	−4.72	−0.12	−5.79	−0.04
	MXN7	−6.10	0.17	−5.68	0.22	−5.38	0.54	−5.95	0.12
	MKN28	−5.89	−0.04	−5.57	0.11	−4.67	−0.17	−5.79	−0.04
	MKN45	−5.85	−0.08	−5.44	−0.02	−4.61	−0.23	−5.83	0.00
	MKN74	−6.63	0.70	−5.85	0.39	−5.25	0.41	−6.24	0.41
Prostate	DU-145	−5.81	−0.12	−4.00	−1.46	−4.63	−0.21	−5.77	−0.06
	PC-3	−5.76	−0.17	−5.16	−0.30	−4.92	0.08	−5.78	−0.05
MG-MID[b]		−5.93		−5.46		−4.83		−5.83	
Delta[c]		0.76		0.39		1.03		0.41	
Range[d]		1.02		1.85		1.45		0.57	

[a] Log concentration of testing compounds for inhibition of cell growth at 50% compared to control.
[b] Arithmetical mean value of log GI_{50} over all cell lines tested.
[c] The difference in log GI_{50} value of the most sensitive cell and MG-MTD value.
[d] The difference in log GI_{50} value of the most sensitive cell and the least sensitive cell.

for the total inhibition of cell growth, and the LC_{50} value, the molar concentration of 50% cell death, were also calculated as $100 \times [(T - T_0)/(C - T_0)] = 0$ and −50, respectively. The detailed measuring procedure of the cell growth inhibition according to the sulforohdamine B assay was described in the cited references.

Based on the assessment of the anti-tumor activity of **13–16** against a variety of human cancer cells using a panel of 39 human cancer cell lines (Table 1), it was determined that RID-B (**13**) strongly inhibited the growth of various cancer cell lines at low concentrations (MG-MID = −5.93). Furthermore, **13** potently inhibited the growth of several cancer cell lines at concentrations of less than 1 μM (at 0.38 μM [MG = −6.42] for SF-539, at 0.58 μM [MG = −6.23] for HT-29, at 0.20 μM [MG = −6.69] for DMS114, at 0.21 μM [MG = −6.67] for LOX-IMVI, at 0.23 μM [MG = −6.63] for MKN74).

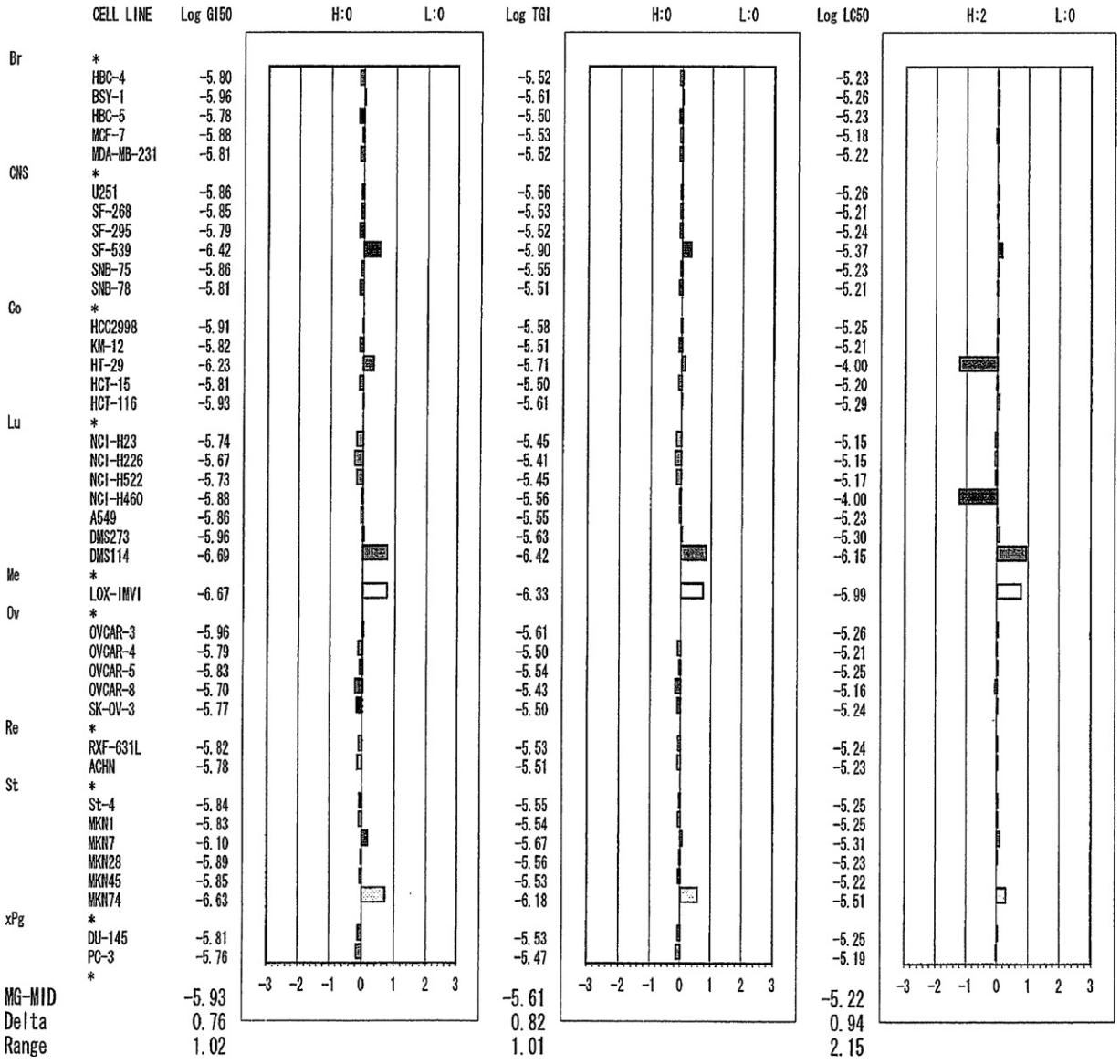

Fig. 8 – Growth inhibition against a panel of 39 human cancer cell lines. The mean graph was produced by computer processing of the GI_{50}s as described in Section 2. The log GI_{50} for each cell line is indicated. *Columns* extending to the *right*, sensitivity to RID-B (13); *columns* extending to the *left*, resistance to RID-B (13). One scale represents one logarithm difference. MG-MID, the mean of log GI_{50} values for 39 cell lines. *Delta*, the logarithm of difference between the MG-MID and the log GI_{50} of the most sensitive cell line. *Range*, the logarithm of difference between the log GI_{50} of the most resistant cell line and the log GI_{50} of the most sensitive one.

4. Discussion

We investigated the cell growth inhibition profile of RID derivatives **13–16** using the human cancer cell line panel. As depicted in Figs. 8–11, the mean graph of **13–16** based on the growth-inhibition parameter of GI_{50} showed the potency of anti-cancer effects of these compounds. Especially, RID-B (**13**) showed differential growth inhibition, and it seemed to be more effective against lung cancer DMS114, melanoma LOX-IMVI, and stomach cancer MKN74 cell lines.

Arithmetical mean value of log GI_{50}, TGI, and log LC_{50} derived from the human cancer cell panel assay are summarized in Table 2. The MG-MID value of log GI_{50} of **13–16** is −5.93 (1.2 μM), −5.46 (3.5 μM), −4.84 (14.5 μM), or −5.83 (1.5 μM), respectively. These parameters showed that effective anti-proliferation concentrations of **13**, **14**, and **16** were sufficiently low. Among them, **13** strongly inhibited the growth of several cancer cell lines at concentrations of less than 1 μM (at 0.38 μM for SF-539 [central nervous system], at 0.58 μM for HT-29 [colon], at 0.20 μM for DMS114 [lung], at 0.21 μM for LOX-IMVI [melanoma], at 0.23 μM for MXN74 [stomach]). Furthermore, **13** also had a significant inhibition activity against cancer cell lines for the breast and ovary (at 1.10 μM for BSY-1 [breast], at 1.10 μM for OVCAR-3 [ovarian]).

We performed an additional experiment using RID-B (**13**) against a normal cell line, the human lung fibroblast MRC-5.

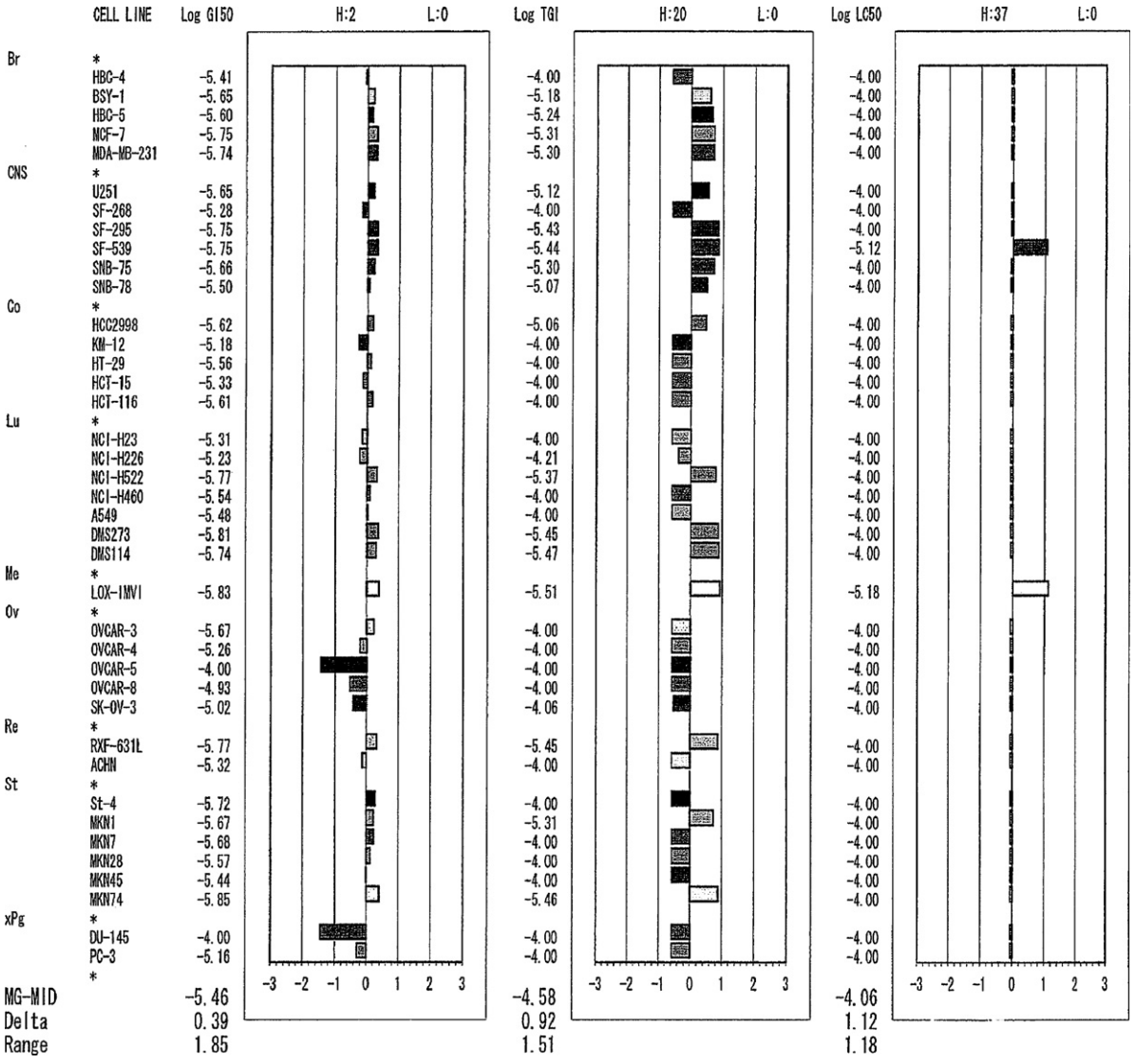

Fig. 9 – Growth inhibition against a panel of 39 human cancer cell lines. The mean graph was produced by computer processing of the GI_{50}s as described in Section 2. The log GI_{50} for each cell line is indicated. *Columns* extending to the *right*, sensitivity to RID-C (14); *columns* extending to the *left*, resistance to RID-C (14). One scale represents one logarithm difference. MG-MID, the mean of log GI_{50} values for 39 cell lines. *Delta*, the logarithm of difference between the MG-MID and the log GI_{50} of the most sensitive cell line. *Range*, the logarithm of difference between the log GI_{50} of the most resistant cell line and the log GI_{50} of the most sensitive one.

Table 2 – Calculated parameters from the human cancer cell line panel assay of *pseudo*-symmetrical tamoxifens 13–16

Compound	Log GI_{50} (M)		Log TGI (M)		Log LC_{50} (M)		Most sensible cell lines
	MG-MID[a]	Range	MG-MID[a]	Range	MG-MID[a]	Range	
RID-B (**13**)	−5.93	−6.69 to −5.67	−5.61	−6.42 to −5.41	−5.22	−6.15 to −4.00	Lung cancer DMS114, melanoma LOX-IMVI, stomach cancer MKN74
RID-C (**14**)	−5.46	−5.85 to −4.00	−4.58	−5.51 to −4.00	−4.06	−5.18 to −4.00	Stomach cancer MKN74, lung cancer DMS273
RID-D (**15**)	−4.84	−5.86 to −4.41	−4.36	−4.91 to −4.00	−4.05	−4.25 to −4.00	Colon cancer HT-29, breast cancer HBC-5
Bis(dimethylamino-phenetole) (**16**)	−5.83	−6.24 to −5.67	−5.50	−5.70 to −5.35	−5.19	−5.30 to −5.02	Stomach cancer MKN74, colon cancer HT-29

[a] Arithmetical mean value of log GI_{50}, log TGI, and log LC_{50} over all cell lines tested.

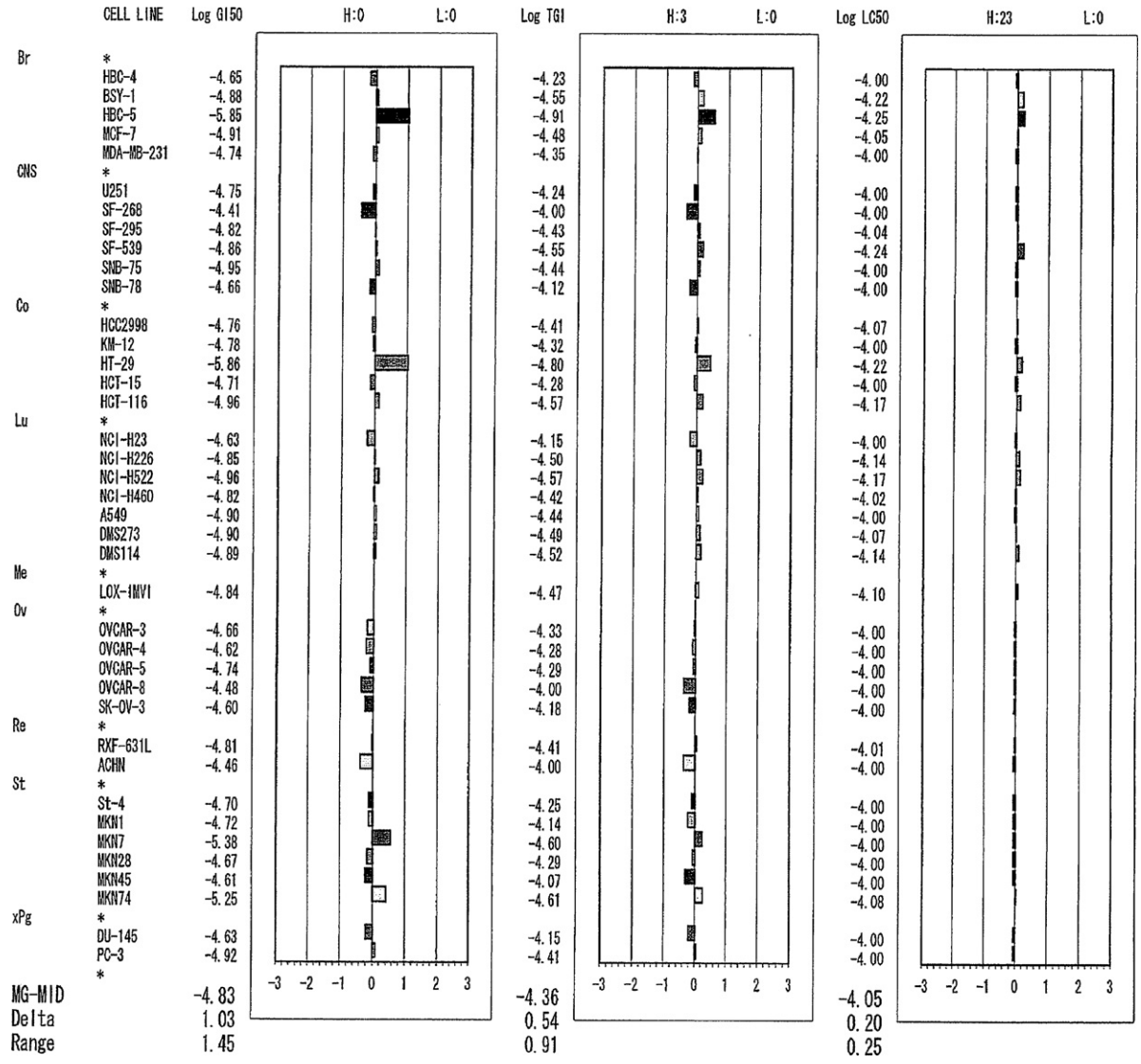

Fig. 10 – Growth inhibition against a panel of 39 human cancer cell lines. The mean graph was produced by computer processing of the GI_{50}s as described in Section 2. The log GI_{50} for each cell line is indicated. *Columns* extending to the *right*, sensitivity to RID-D (15); *columns* extending to the *left*, resistance to RID-D (15). One scale represents one logarithm difference. MG-MID, the mean of log GI_{50} values for 39 cell lines. *Delta*, the logarithm of difference between the MG-MID and the log GI_{50} of the most sensitive cell line. *Range*, the logarithm of difference between the log GI_{50} of the most resistant cell line and the log GI_{50} of the most sensitive one.

Based on the sulforhodamine B assay, the GI_{50} value of RID-B for MRC-5 was determined to be 4.14 μM when using 5% FBS. The GI_{50} concentrations of **13** to anti-tumor cell lines varied from 0.2 to 2 μM and the average GI_{50} value was 1.2 μM as shown in Table 1, therefore, the dose for MRC-5 is much higher than that of the average value of 39 cancer cell lines. This result suggests that **13** tends to affect cancer cells more than non-malignant cells. However, further studies using other normal cells and *in vivo* models are needed to evaluate the effect of **13** on normal cells.

We have already established a method to compare the cell growth inhibition profiles against the JFCR 39 (so-called fingerprints) of more than 200 standard drugs including tamoxifen, toremifene, chromifene, paclitaxel (Taxol), doxorubicin, fluorouracil, cytarabine, methotrexate, vincristine, cisplatin, and irinotecan using the COMPARE analysis [25–30], and it was shown that the COMPARE analysis is an information-intensive approach to identify the molecular targets of a new compound, as descried by Paull and coworkers [33] and Paull et al. [34]. The evaluated system can be used to predict the molecular target or the mode of action of the test compounds by assessing the correlation coefficient between the fingerprints of test compounds and various reference compounds with known modes and action.

The profiles of the difference in the log GI_{50} and MG-MID values of **13–16** (Figs. 8–11) were compared with those of 200 standard compounds using the COMPARE Program. The COMPARE Program that evaluated the pattern of differential growth inhibition of **13–16** showed a weak correlation with that of the other drugs as shown in Table 3. It was revealed that

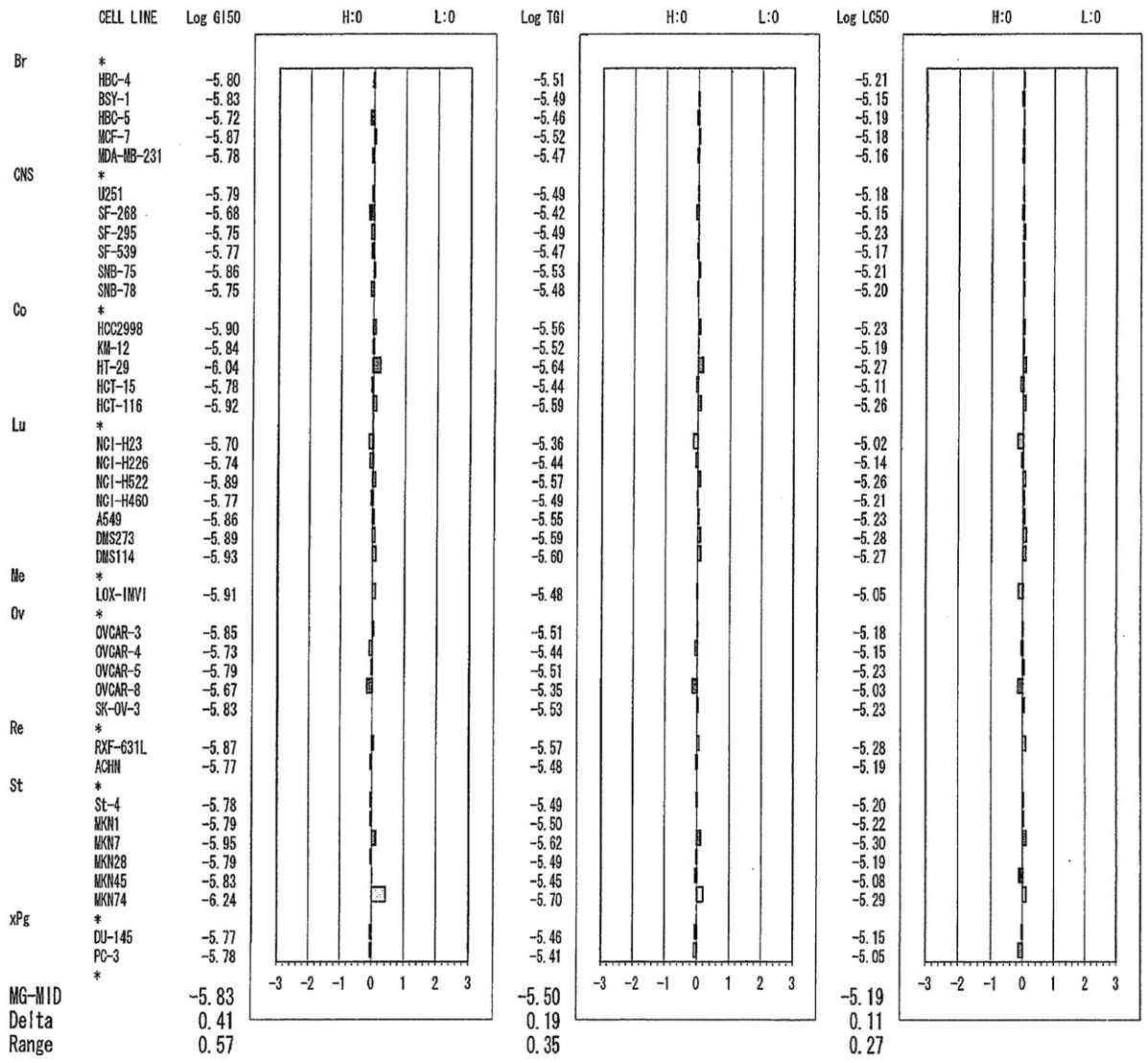

Fig. 11 – Growth inhibition against a panel of 39 human cancer cell lines. The mean graph was produced by computer processing of the GI_{50}s as described in Section 2. The log GI_{50} for each cell line is indicated. *Columns* extending to the *right*, sensitivity to bis(dimethylaminophenetole) (16); *columns* extending to the *left*, resistance to bis(dimethylaminophenetole) (16). One scale represents one logarithm difference. MG-MID, the mean of log GI_{50} values for 39 cell lines. *Delta*, the logarithm of difference between the MG-MID and the log GI_{50} of the most sensitive cell line. *Range*, the logarithm of difference between the log GI_{50} of the most resistant cell line and the log GI_{50} of the most sensitive one.

the fingerprints of **13** and **16** correlated with the fingerprints of the no anti-cancer drug currently in use (Peason correlation coefficient [*r*] compared with all the reference compounds is <0.5). On the other hand, the COMPARE analysis of the mean graph revealed that derivatives **14** and **15** correlated slightly with tamoxifen (**1**), an estrogen-type anti-cancer agent ($r = 0.551$ and 0.523). From these results, it has been postulated that the molecular binding targets of **14** and **15** are identical to those of tamoxifen, but that the targets of **16**, and especially **13**, are quite different from those of tamoxifen. Tamoxifen binds to the estrogen receptor (ER) and inhibits cell proliferation. In the COMPARE analysis, we used 39 human cancer cell lines including the ER-positive cell lines (such as MCF-7, SK-OV-3, and PC-3) and ER-negative cell lines (such as MDA-MB-231, OVCAR-5, and DU-145), and **13** inhibited the cell growth of all cancer cells at similar doses, suggesting that the expression state of ER is not related to the cell growth inhibition. Furthermore, in our recent study, **13**-induced rapid (>4 h) mitochondria-involved cell death to the ER-negative human leukemia cell line Jurkat (data not shown). These results suggested that **13** and **16** might be potent candidates as anti-tumor agents with modes of action different from those of existing cancer treatment drugs. However, we cannot completely exclude the possibility that **13** and **16** might bind to the ER.

In summary, we developed the effective synthesis of new anti-tumor agents, i.e., *pseudo*-symmetrical tamoxifen derivatives RID-B (**13**), RID-C (**14**), RID-D (**15**), and bis(dimethylaminophenetole) (**16**) from very simple molecules in a four-step synthesis. Although **15** (involving morpholine part) does not

Table 3 – The COMPARE analysis of 13–16

Compound	Ranking order	Drug	r^a
RID-B (**13**)	1	6-Mercaptopurine	0.455
	2	Cisplatin	0.453
	3	Doxifluridine	0.448
RID-C (**14**)	1	Tamoxifen	0.551
	2	PSC833	0.537
	3	PSC833	0.455
RID-D (**15**)	1	Tamoxifen	0.523
	2	HCFU	0.509
	3	Tamoxifen	0.421
Bis(dimethylamino-phenetole) (**16**)	1	Toremifene	0.473
	2	Tamoxifen	0.467
	3	Actinomycin-D	0.393

The mean graph of **13–16** was compared with those of 200 standard compounds using the COMPARE analysis. Drugs were ordered according to the correlation coefficient. Drugs with correlation coefficients higher than 0.5 ($P < 0.001$) were included.
[a] Peason correlation coefficient.

have any biological activity during the MTT assay, **13** (involving pyrrolidine moiety), **14** (involving piperidine moiety), and **16** (involving dimethylamino moiety) showed significant anti-tumor activities against the HL-60 human acute promyelocytic leukemia. It was also discovered that the time-dependent activity of **13** is superior to those of **14** and **16** as depicted in Fig. 3.

According to the assessment of the global anti-tumor activity of **13–16** against a variety of human cancer cells using a panel of 39 human cancer cell lines, it was shown that RID-B (**13**) strongly inhibited the growth of several cancer cell lines, such as SF-539, HT-29, DMS114, LOX-IMVI, and MKN74, at low concentrations. The *pseudo*-symmetrical compound **13** might be potent candidates as anti-tumor agents with different modes of action from existing drugs for cancer treatment because the COMPARE computer algorithm showed a low correlation between the fingerprint of **13** to those of the established anti-cancer drugs. The synthesis of other derivatives and further studies of the anti-tumor activities of these new entries as *pseudo*-symmetrical tamoxifen agents are now in progress.

Acknowledgments

This work was partially supported by the Science Research Promotion Fund from the Promotion and Mutual Aid Corporation for Private Schools of Japan, and a Research Grant from the Center for Green Photo-Science and Technology.

Appendix A. Supplementary data

Supplementary data associated with this article can be found, in the online version, at doi:10.1016/j.bcp.2007.11.005.

REFERENCES

[1] Catherino WH, Jordan VC. A risk-benefit assessment of tamoxifen therapy. Drug Safe 1993;8:381–97.
[2] Evans GL, Turner RT. Tissue-selective actions of estrogen analogs. Bone 1995;17:181S–90S.
[3] Fisher B, Costantino JP, Wickerham DL, Redmond CK, Kavanah M, Cronin WM, et al. Tamoxifen for prevention of breast cancer: report of the national surgical adjuvant breast and bowel project P-1 study. J Natl Cancer Inst 1998;90:1371–88.
[4] Gradishar WJ, Jordan VC. Clinical potential of new antiestrogens. J Clin Oncol 1997;15:840–52.
[5] Jordan VC. Antiestrogens and selective estrogen receptor modulators as multifunctional medicines. 2. Clinical considerations and new agents. J Med Chem 2003;46:1081–111.
[6] Lonard DM, Smith CL. Molecular perspectives on selective estrogen receptor modulators (SERMs): progress in understanding their tissue-specific agonist and antagonist actions. Steroids 2002;67:15–24.
[7] McDonnell DP. The molecular pharmacology of SERMs. Trends Endcrin Metabol 1999;10:301–11.
[8] Preliminary communication: Shiina I, Sano Y, Nakata K, Kikuchi T, Sasaki A, Ikekita M, et al. Synthesis of the new *pseudo*-symmetrical tamoxifen derivatives and their anti-tumor activity. Bioorg Med Chem Lett 2007;17:2421–4.
[9] Shiina I, Suzuki M. The catalytic Friedel-Crafts alkylation reaction of aromatic compounds with benzyl or allyl silyl ethers using $Cl_2Si(OTf)_2$ or $Hf(OTf)_4$. Tetrahedron Lett 2002;43:6391–4.
[10] Shiina I, Suzuki M, Yokoyama K. A convenient method for the synthesis of 4,4-diarylbut-1-enes via the successive allylation of aromatic aldehydes and the Friedel-Crafts alkylation reaction of anisole with the intermediary benzyl silyl ethers using $HfCl_4$ or $Cl_2Si(OTf)_2$. Tetrahedron Lett 2002;43:6395–8.
[11] Shiina I, Suzuki M, Yokoyama K. Short-step synthesis of tamoxifen and its derivatives *via* the three-component coupling reaction and migration of the double bond. Tetrahedron Lett 2004;45:965–7.
[12] For the instances of tamoxifen synthesis recently reported. See: Zhou C, Larock RC. Regio- and stereoselective route to tetrasubstituted olefins by the palladium-catalyzed three-component coupling of aryl iodides, internal alkynes, and arylboronic acids. J Org Chem 2005;70:3765–77. and references cited therein.
[13] Sano Y, Shiina I. Short-step synthesis of droloxifene via the three-component coupling reaction among aromatic aldehyde, cinnamyltrimethylsilane, and β-chlorophenetole. Tetrahedron Lett 2006;47:1631–5.
[14] Sano Y, Nakata K, Otoyama T, Umeda S, Shiina I. An expeditious synthesis of lasofoxifene and nafoxidine via the novel three-component coupling reaction. Chem Lett 2007;36:40–1.
[15] Schneider MR, von Angerer E, Schönenberger H, Michel RT, Fortmeyer HP. 1,1,2-Triphenylbut-1-enes: relationship between structure, estradiol receptor affinity, and mammary tumor inhibiting properties. J Med Chem 1982;25:1070–7.
[16] Stoessel S, Leclercq GJ. Competitive binding assay for estrogen receptor in monolayer culture: measure of receptor activation potency. Steroid Biochem 1986;25:677–82.
[17] Schneider MR, Hartmann RW, Sinowatz F, Amselgruber W. Nonsteroidal antiestrogen and partial estrogens with prostatic tumor inhibition activity. J Cancer Res Clin Oncol 1986;112:258–65.

[18] Schuderer ML, Schneider MR. Cytotoxic esters of 1,1-bis-(4-hydroxyphenyl)-2-phenyl-but-1-ene with selective antitumor activity against estrogen receptor-containing mammary tumors. J Cancer Res Clin Oncol 1987;113:230–4.
[19] Gyling M, Leclercq G. Estrogen and antiestrogen interaction with estrogen receptor of MCF-7 cells-relationship between processing and estrogenicity. J Steroid Biochem 1988; 29:1–8.
[20] Lubczyk V, Bachmann H, Gust R. Investigation on estrogen receptor binding. The estrogenic, antiestrogenic, and cytotoxic properties of C2-alkyl-substituted 1,1-bis(4-hydroxyphenyl)-2-phenylethenes. J Med Chem 2002;45:5358–64.
[21] Laïos I, Journe F, Laurent G, Nonclercq D, Toillon RA, Seo HS, et al. Mechanisms governing the accumulation of estrogen receptor alpha in MCF-7 breast cancer cells treated with hydroxytamoxifen and related antiestrogens. J Steroid Biochem Mol Biol 2003;87:207–21.
[22] Yu DD, Forman BM. Simple and efficient production of (Z)-4-hydroxytamoxifen, a potent estrogen receptor modulator. J Org Chem 2003;68:9489–91.
[23] Vessières A, Top S, Pigeon P, Hillard E, Boubeker L, Spera D, et al. Modification of the estrogenic properties of diphenols by the incorporation of ferrocene. Generation of antiproliferative effects in vitro. J Med Chem 2005; 48:3937–40.
[24] Stanciuc O, Niculescu-Duvaz I, Stanciuc G, Balaban AT. Clomiphene and tamoxifen analogues as potential non-steroidal antiestrogens. Rev Roum Chim 1997;42:733–41.
[25] Dan S, Tsunoda T, Kitahara O, Yanagawa R, Zembutsu H, Katagiri T, et al. An integrated database of chemosensitivity to 55 anticancer drugs and gene expression profiles of 39 human cancer cell lines. Canser Res 2002;62:1139–47.
[26] Yamori T. Panel of human cancer cell lines provides valuable database for drug discovery and bioinformatics. Cancer Chemother Pharmacol 2003;52(Suppl 1):S74–9.
[27] Yamori T, Matsunaga A, Sato S, Yamazaki K, Komi A, Ishizu K, et al. Potent antitumor activity of MS-247, a novel DNA minor groove binder, evaluated by an in vitro and in vivo human cancer cell line panel. Cancer Res 1999;59:4042–9.
[28] Yaguchi S, Fukui Y, Koshimizu I, Yoshimi H, Matsuno T, Gouda H, et al. Antitumor activity of ZSTK474, a new phosphatidylinositol 3-kinase inhibitor. J Natl Cancer Inst 2006;98:545–56.
[29] Nakatsu N, Yoshida Y, Yamazaki K, Nakamura T, Dan S, Fukui Y, et al. Chemosensitivity profile of cancer cell lines and identification of genes determining chemosensitivity by an integrated bioinformatical approach using cDNA arrays. Mol Cancer Ther 2005;4:399–412.
[30] Nakatsu N, Nakamura T, Yamazaki K, Sadahiro S, Makuuchi H, Kanno J, et al. Evaluation of action mechanisms of toxic chemicals using JFCR39, a panel of human cancer cell lines. Mol Pharmacol 2007;72:1171–80.
[31] Fidler IJ. Biological behavior of malignant melanoma cells correlated to their survival in vivo. Cancer Res 1975; 35:218–24.
[32] Skehan P, Storeng R, Scudiero D, Monks A, McMahon J, Vistica D, et al. New colorimetric cytotoxicity assay for anticancer-drug screening. J Natl Cancer Inst 1990;82: 1107–12.
[33] Monks A, Scudiero D, Skehan P, Shoemaker R, Paull K, Vistica D, et al. Feasibility of a high-flux anticancer drug screen using a diverse panel of cultured human tumor cell lines. J Natl Cancer Inst 1991;83:757–66.
[34] Paull KD, Shoemaker RH, Hodes L, Monks A, Scudiero DA, Robinstein K, et al. Display and analysis of patterns of differential activity of drugs against human tumor cell lines: development of mean graph and COMPARE algorithm. J Natl Cancer Inst 1989;81:1088–92.
[35] Boyd MR. Status of the National Cancer Institute preclinical antitumor drug discovery screen in implications for selection of new agents for clinical trial, vol. 3. Philadelphia, PA: Lippincott; 1989.
[36] Robertson DW, Katzenellenbogen JA, Hayes JR, Katzenellenbogen BS. Antiestrogen basicity-activity relationships: a comparison of the estrogen receptor binding and antiuterotrophic potencies of several analogues of (Z)-1,2-diphenyl-1-[4-[2-(dimethylamino)ethoxy]phenyl]-1-butene (tamoxifen, nolvadex) having altered basicity. J Med Chem 1982;25:167–71.
[37] Dayan G, Lupien M, Auger A, Anghel SI, Rocha W, Croisetière S, et al. Tamoxifen and raloxifene differ in their functional interactions with aspartate 351 of estrogen receptor α. Mol Pharmacol 2006;70:579–88.
[38] Agouridas V, Laïos I, Cleeren A, Kizilian E, Magnier E, Blazejewski JC, et al. Loss of antagonistic activity of tamoxifen by replacement of one *N*-methyl of its side chain by fluorinated residues. Bioorg Med Chem 2006;14:7531–8.